Controlling the Phase Content of Li_2O-Al_2O_3-SiO_2-B_2O_3-BaO Glass-Ceramic Bonds with CTE Close to cBN

Zichen Guo
"Wuhan University of Technology"
Feng He (he-feng2002@163.com)
Wuhan University of Technology
Zuhao Li
Wuhan University of Technology
Dongyang Yan
Wuhan University of Technology
Junlin Xie
Wuhan University of Technology

Research Article

Keywords: Glass-ceramics, CTE, cBN, Phase content, Sintering, Composite materials

Posted Date: September 18th, 2020

DOI: https://doi.org/10.21203/rs.3.rs-78062/v1

Abstract

Li_2O-Al_2O_3-SiO_2-B_2O_3-BaO glass-ceramic bonds with CTE close to cBN for vitrified cBN composites was prepared via a two-step heat treatment method. The crystalline phases were identified by XRD and the phase content was analyzed by WPF refinement. The increasing crystallization temperature would promote the precipitation of more $LiAlSi_3O_8$ phase in the glass-ceramic, which was conducive to the preparation of low CTE glass-ceramics. Besides, a crystallization temperature below 625 °C was necessary for the preparation of Li_2O-Al_2O_3-SiO_2-B_2O_3-BaO glass-ceramic with CTE close to cBN (3.50×10^{-6} °C^{-1}), proving that the two-step heat treatment was an effective sintering process to the preparation of low CTE glass-ceramic bonds for vitrified cBN composites.

1 Introduction

Glass-ceramic bonds, which can effectively consolidate the superhard abrasives into a fixed shape after a sintering process, are considered as one of the most important components of the modern vitrified superhard abrasive tools. Among the few studied glass-ceramic bonds, lithium aluminosilicate glass-ceramic is outstanding for its adjustable CTE in a wide temperature range[1], low liquid phase formation temperature[2], and high bending strength[3]. In this regard, Li_2O-Al_2O_3-SiO_2-B_2O_3-BaO glass-ceramic with a CTE of 5.34×10^{-6} °C^{-1} sintered at 860 °C for 2 h was supposed to be promising for vitrified composites[4]. However, since the CTE of cBN (Cubic Boron Nitride) is 3.50×10^{-6} °C^{-1}[5], and it is well known that the closer the CTE of the glass-ceramic is to cBN, the less microcracks between the bonds and cBN particles caused by the mismatched CTE of these two parts during the natural cooling of the sintering process for vitrified composites will generate, which ensure the preparation of abrasive tools with high performances. Actually, the CTE of glass-ceramic could be controlled by the type and content of precipitated crystalline phases[6]. Besides, in addition to the varying in the composition of the glass-ceramic bonds, the changing in heat treatments performed on the bonds also has a great influence on the type and content of crystalline phases in glass-ceramic bonds which will make considerable differences on the performances of bonds and superhard abrasive tools[7]. To date, two different sintering process are frequently-used for the preparation of glass-ceramic: one-step heat treatment method[8] and two-step heat treatment method[9]. The most obvious difference between these two heat treatment method is that the sintering and crystallization processes are carried out at different temperature in two-step heat treatment method, which is beneficial to the elimination of pores and the precipitation of crystalline phases in glass-ceramic[10]. In this paper, a two-step heat treatment method was applied to prepare Li_2O-Al_2O_3-SiO_2-B_2O_3-BaO glass-ceramic with CTE close to cBN.

2 Experimental

2.1 Materials preparation

The parent glass with chemical composition shown in Table 1 was synthesized through melting mixed raw materials at 1500 °C for 2 h and then quenching the acquired melts into ice water. Then, the obtained parent glasses were dried and ground to pass through 240 mesh sieves before they were pressed into rectangular bars (40 mm × 6 mm × 5 mm) with the assistance of 5% PVA solution under 30 MPa of pressure.

Table 1
Chemical compositions of glass

Oxide	SiO_2	B_2O_3	BaO	Li_2O	Al_2O_3	CaO	Na_2O	MgO	others
wt.%	54.00	10.00	9.00	6.00	10.00	2.00	3.00	3.00	3.00

In this study, the pressed parent glasses were first sintered at 860 °C for 2 h with a heating rate of 5 °C/min starting from room temperature. Then, the sintered samples were cooled down to crystallization temperature at a cooling rate of 2.5 °C/min from 860 °C and held for 1 h at the crystallization temperature before they were furnace-cooled to room temperature. The crystallization temperatures were set as 550 °C, 575 °C, 600 °C, and 625 °C for M1, M2, M3, and M4, respectively.

2.2 Materials characterization

An X-ray diffraction (XRD, D8 Advance, Bruker, Germany) was employed to identify the crystalline phases of as-quenched glasses and M1-M4 glass-ceramic at a scanning rate of 2 °/min from 10 °-80 °with utilizing Cu Kα radiation source. In addition, CTEs of sintered strip glass-ceramics were measured by a thermal dilatometer (DIL-402C, NETZSCH, Germany) with a heating rate of 5 °C/min from room temperature to 600 °C. In order to quantify the content of crystalline phase for glass-ceramics, Whole Pattern Fitting (WPF) refinement was carried out using "MDI JADE 6" software.

3 Results And Discussions

Figure 1 showed the XRD pattern of as-quenched glass and glass-ceramics. It could be seen that no crystalline phases had been precipitated in the prepared parent glass. However, $LiAlSi_2O_6$ and $LiAlSi_3O_8$ constituted as the major crystalline phases were precipitated in the prepared glass-ceramics. Besides, Li_2SiO_3 and $BaAl_2Si_2O_8$ were identified as the minor crystalline phases. An overall analysis of Fig. 1 could reach the conclusion that the changing of crystallization temperature made no difference to the type of crystalline phase precipitated in the glass-ceramics.

Figure 2 displayed that the CTE of glass-ceramic crystallized at 550 °C was 2.91×10^{-6} °C^{-1}, and it was 3.13×10^{-6} °$C^{-1}$and 3.11×10^{-6} °C^{-1} when the crystallization temperature increased to 575 °C and 600 °C, respectively. However, the CTE of glass-ceramic had reduced to 2.58×10^{-6} °C^{-1} with a rising crystallization temperature to 625 °C, indicating a higher crystallization temperature was not conducive to the preparation of with CTE close to cBN (3.50×10^{-6} °C^{-1}).

To explore the type and content of crystalline phases on the performance of CTE for glass-ceramics, a theoretical calculation method of CTE was adopted[11].

$$\alpha_{gc} = x_g\alpha_g + x_{c1}\alpha_{c1} + x_{c2}\alpha_{c2} + x_{c3}\alpha_{c3} + x_{c4}\alpha_{c4} \quad (1)$$

Where α_{gc} denotes the calculated CTE of glass-ceramics, α_g, α_{c1}, α_{c2}, α_{c3}, and α_{c4} stands for the CTE of residual amorphous phase, $LiAlSi_2O_6$ ($0.9 \times 10^{-6}\ °C^{-1}$)[12], $LiAlSi_3O_8$ ($3 \times 10^{-6}\ °C^{-1}$)[13], Li_2SiO_3 ($9.0 \times 10^{-6}\ °C^{-1}$)[14], and $BaAl_2Si_2O_8$ ($2.2 \times 10^{-6}\ °C^{-1}$)[15], respectively. While the x_g, x_{c1}, x_{c2}, x_{c3}, and x_{c4} represents the content of the above-mentioned phases.

In Eq. (1), the CTE of the residual amorphous phase could be determined as $7.69 \times 10^{-6}\ °C^{-1}$ by the chemical compositions of glass shown in Table 1 according to the Appen method[16]. In addition, the phase content in glass-ceramics could be obtained by WPF refinement of XRD pattern, and the calculated and measured CTE of glass-ceramics, as well as the phase content in glass-ceramics, were depicted in Fig. 3.

As Fig. 3 pointed out that the calculated and measured CTEs of glass-ceramics were close to each other, indicating that the calculated method of CTEs for glass-ceramics in this paper were suitable and effective. The crystallinity of the glass-ceramic continued to increase with a rising crystallization temperature. As for the content of major crystalline phases in glass-ceramics, the phase content of $LiAlSi_2O_6$ reached its maximum in M1 among the four samples which was 63.25%, while it was 51.90%~53.55% for the rest crystallization temperatures, proving that the precipitation of $LiAlSi_2O_6$ was almost unaffected when the crystallization temperature was among 575 ~ 625 °C. Furthermore, the phase content of $LiAlSi_3O_8$ kept increasing with the rising crystallization temperature indicating that the precipitation of $LiAlSi_3O_8$ was inspired at a higher crystallization temperature. Actually, the transition temperature of nucleation from crystallization temperature for $LiAlSi_3O_8$ was lower than that of $LiAlSi_2O_6$[17], demonstrating that the high crystallization temperature was more favorable for the precipitation of $LiAlSi_3O_8$. Thus, a higher content of crystalline phase and $LiAlSi_3O_8$ in M4 could be reasonably explained. While it could be seen that the CTEs of $LiAlSi_2O_6$ and $LiAlSi_3O_8$ were obviously lower than the amorphous phase. Hence, a higher content of $LiAlSi_2O_6$ and $LiAlSi_3O_8$, as well as a lower content of the amorphous phase, could be beneficial for a lower CTE of M4 glass-ceramic according to Eq. (1). However, since the CTE of cBN was $3.50 \times 10^{-6}\ °C^{-1}$, the difference between M4 and cBN in CTE was also too large to the formation of microcracks aroused by the mismatch of cBN and glass-ceramic bond. In brief, rational control of the crystallization temperature for the two-step heat treatment method can adjust the relative content of $LiAlSi_2O_6$ and $LiAlSi_3O_8$, thereby preparing a glass-ceramic with CTE close to cBN.

4 Conclusion

A two-step heat treatment method had been provided to be an effective sintering process to the preparation of low CTE glass-ceramic bonds for vitrified cBN composites. The increasing crystallization temperature would promote the precipitation of more $LiAlSi_3O_8$ phase in the glass-ceramic, which was conducive to the preparation of low CTE glass-ceramics. Besides, a crystallization temperature below 625 °C was necessary for the preparation of Li_2O-Al_2O_3-SiO_2-B_2O_3-BaO glass-ceramic with CTE close to cBN via a two-step heat treatment.

5 Declaration

Acknowledge

The authors wish to express their sincere gratitude to Yumei Li, the Material Research and Testing Center of Wuhan University of technology.

6 References

1. Soares V O, Peitl O, Zanotto E D. New Sintered-Al_2O_3-SiO_2 Ultra-Low Expansion Glass-Ceramic[J]. Journal of the American Ceramic Society. 2013, 96(4): 1143-1149.
2. Li B, Qing Z, Li Y, et al. Effect of CaO content on structure and properties of low temperature co-fired glass-ceramic in the Li_2O-Al_2O_3-SiO_2 system[J]. Journal of Materials Science: Materials in Electronics. 2016, 27(3): 2455-2459.
3. Qing Z. The effects of B_2O_3 on the microstructure and properties of lithium aluminosilicate glass-ceramics for LTCC applications[J]. Materials Letters. 2018, 212: 126-129.
4. Shi J, He F, Xie J, et al. Effect of heat treatments on the Li_2O-Al_2O_3-SiO_2-B_2O_3-BaO glass-ceramic bond and the glass-ceramic bond cBN grinding tools[J]. International Journal of Refractory Metals and Hard Materials. 2019, 78: 201-209.
5. Bello I, Chong Y M, Leung K M, et al. Cubic boron nitride films for industrial applications[J]. Diamond and Related Materials. 2005, 14(11): 1784-1790.
6. Pisciella P, Pelino M. Thermal expansion investigation of iron rich glass-ceramic[J]. Journal of the European Ceramic Society. 2008, 28(16): 3021-3026.
7. Zhang Q, Zhu Y, Li Z. Performance investigation of Li_2O-Al_2O_3-$4SiO_2$ based glass-ceramics with B_2O_3, Na_3AlF_6 and Na_2O fluxes[J]. Journal of Non-Crystalline Solids. 2012, 358(3): 680-686.
8. Torres F J, Alarcón J. Effect of additives on the crystallization of cordierite-based glass-ceramics as glazes for floor tiles[J]. Journal of the European Ceramic Society. 2003, 23(6): 817-826.
9. Cheng C, Hsieh T, Lin I. Microwave dielectric properties of glass-ceramic composites for low temperature co-firable ceramics[J]. Journal of the European Ceramic Society. 2003, 23(14): 2553-2558.

10. Lu A X, Ke Z B, Xiao Z H, et al. Effect of heat-treatment condition on crystallization behavior and thermal expansion coefficient of $Li_2O–ZnO–Al_2O_3–SiO_2–P_2O_5$ glass–ceramics[J]. Journal of Non-Crystalline Solids. 2007, 353(28): 2692-2697.
11. Li B, Wang S, Fang Y. Effect of Cr_2O_3 addition on crystallization, microstructure and properties of Li_2O-Al_2O_3-SiO_2 glass-ceramics[J]. Journal of Alloys and Compounds. 2017, 693: 9-15.
12. Arcaro S, Moreno B, Chinarro E, et al. Properties of LZS/nanoAl_2O_3 glass-ceramic composites[J]. Journal of Alloys and Compounds. 2017, 710: 567-574.
13. Laczka M, Laczka K, Cholewa-Kowalska K, et al. Mechanical Properties of a Lithium Disilicate Strengthened Lithium Aluminosilicate Glass-Ceramic[J]. Journal of the American Ceramic Society. 2013, 97(2): 361-364.
14. Laczka M, Laczka K, Cholewa Kowalska K, et al. Mechanical Properties of a Lithium Disilicate Strengthened Lithium Aluminosilicate Glass-Ceramic[J]. Journal of the American Ceramic Society. 2014, 97(2): 361-364.
15. Ye F, Gu J C, Zhou Y, et al. Synthesis of $BaAl_2Si_2O_8$ glass-ceramic by a sol-gel method and the fabrication of SiC_{pl}/$BaAl_2Si_2O_8$ composites[J]. Journal of the European Ceramic Society. 2003, 23(13): 2203-2209.
16. Scholze H. Glass: nature, structure, and properties[M]. Springer Science & Business Media, 2012.
17. Ahamad L, Rakshit S K, Parida S C, et al. Solid-state synthesis and heat capacity measurements of ceramic compounds $LiAlSiO_4$, $LiAlSi_2O_6$, $LiAlSi_3O_8$, and $LiAlSi_4O_{10}$[J]. Journal of Thermal Analysis and Calorimetry. 2013, 112(1): 17-23.

Figures

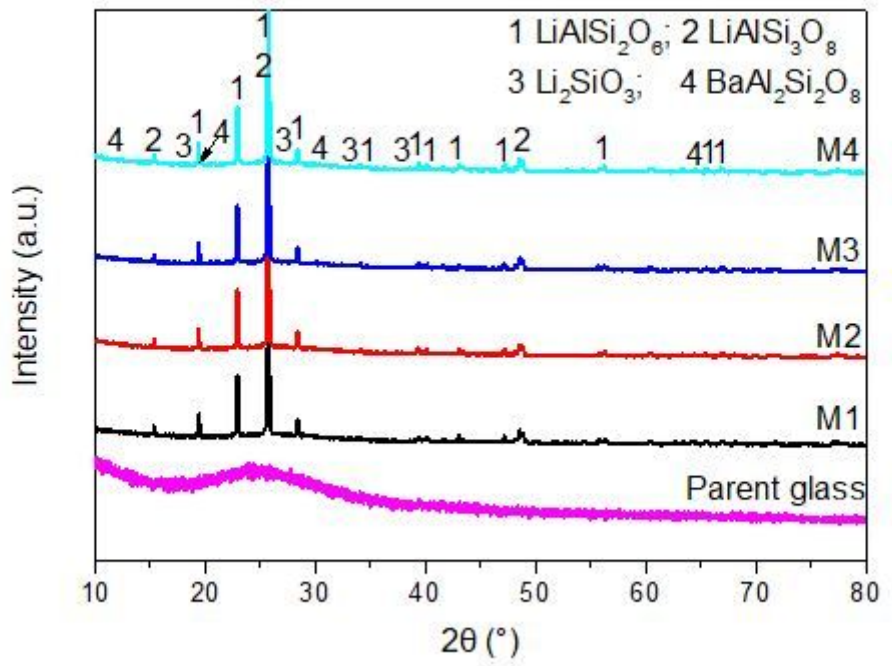

Figure 1

XRD pattern of as-quenched glass and glass-ceramics

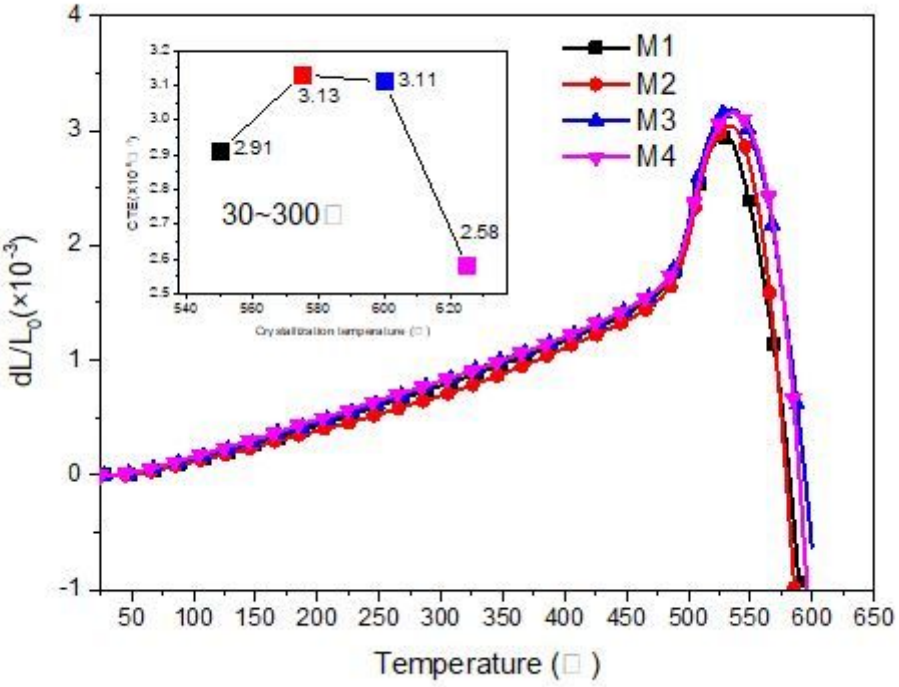

Figure 2

CTE of glass-ceramics prepared at different crystallization temperatures

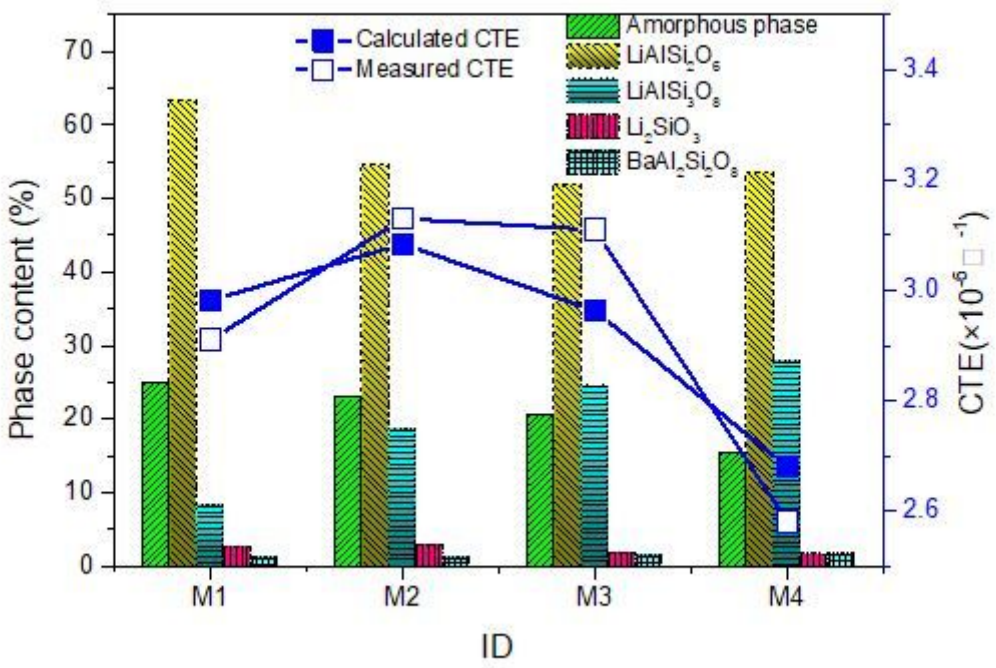

Figure 3

Results of WPF refinement and comparisons between calculated CTE and measured CTE of glass-ceramic